# Implementation of Hagedorn-Brown Correlation Method in Single Fluid Volume Element (SFVE) Method for Predicting Flow of Geothermal Well based on Pressure-Depth and Temperature-Depth Measurement Data at Static Condition

Sparisoma Viridi[1,*], Windra Yusman[2], and Sudjati Rachmat[2]

[1]Nuclear Physics and Biophysics, Faculty of Mathematics and Natural Science,
Institut Teknologi Bandung, Jl. Ganesha 10. Bandung 40132, Indonesia

[2]Geothermal Engineering, Faculty of Mining and Petroleum Engineering,
Institut Teknologi Bandung, Jl. Ganesha 10. Bandung 40132, Indonesia

*dudung@fi.itb.ac.id

**Abstract**. Advancement of implementation of single fluid volume element (SFVE) method in geothermal well application is presented in this work. Static pressure-depth profile is changed to dynamic one by implementing Hagedorn-Brown correlation method, which takes into account effects of acceleration, elevation, and friction in pressure depth calculation. Two-phase flow influences in mass flow, velocity, enthalpy, and density of flow are also considered.

Keywords: finite difference, fluid flow, transient flow, geothermal well, Hagedorn-Brown correlation.

PACS: 47.27.nf, 47.60.-i, 91.40.Ge.

## 1 Introduction

Single fluid volume element (SFVE) method [1] implementation for predicting flow occurrence of a geothermal well based on its static pressure-depth and temperature-depth measurements has been presented in previous work [2], which could be considered as simpler and transient version of method proposed by Poetmann-Carpenter. It is unfortunately required very small density of the fluid volume element in order to match the observations. This unrealistic requirement could be addressed to the static pressure-depth profile that will be dynamic in this work by updating it using pressured drop formulation due to some effects (acceleration, elevation, and friction). Two-phase influence (liquid and gas phase) from Hagedorn-Brown is also considered.

## 2 Theory

In this section all equations involved in Hagedorn-Brown (HB) correlation method are listed and briefly explained, including water saturation condition, water and vapor density (and also enthalpy), and several pressure drop contributions (friction, elevation, and acceleration effects). Two mixture parameter $x$ and $y$ are considered. The former is derived from enthalpy ratio and the later is defined as fraction as volume occupy by liquid in pipe element.

### 2.1 Water properties in liquid and gas phase

Water saturation temperature as function of pressure can be found using following empirical relation

$$T_S = \sum_{n=0}^{4} c_n^{TS} \ln^n p \qquad (1)$$

for $6.11 \times 10^2$ Pa $\leq p \leq 2.212 \times 10^7$ Pa, with value of the constants are listed in Table 1.

Table 1. Constants in Equation (1).

| $n$ | $c_n^{TS}$ |
|---|---|
| 0 | $2.80034 \times 10^2$ |
| 1 | $1.40856 \times 10^1$ |
| 2 | $1.38075 \times 10^0$ |
| 3 | $-1.01806 \times 10^{-1}$ |
| 4 | $1.9017 \times 10^{-2}$ |

Term ln in Equation (1) stands for natural logarithmic function.

Liquid density of water follows

$$\rho_L = \sum_{n=0}^{5} c_n^{\rho L} T^n \qquad (2)$$

for 273.15 K $\leq T \leq$ 640 K, with the constants are given in Table 2.

Table 2. Constants in Equation (2).

| $n$ | $c_n^{\rho L}$ |
|---|---|
| 0 | $3.78631 \times 10^3$ |
| 1 | $-3.72487 \times 10^1$ |
| 2 | $1.96246 \times 10^{-1}$ |
| 3 | $-5.04708 \times 10^{-4}$ |
| 4 | $6.29368 \times 10^{-7}$ |
| 5 | $-3.0848 \times 10^{-9}$ |

Density of vapor or water in gas phase follows

$$\rho_G = \exp\left( \sum_{n=0}^{5} c_n^{\rho G} T^n \right) \qquad (3)$$

for 273.15 K $\leq T \leq$ 645 K, where Table 3 gives value of the constants.

Table 3. Constants in Equation (3).

| $n$ | $c_n^{\rho G}$ |
|---|---|
| 0 | -9.37072 × 10$^1$ |
| 1 | 8.33941 × 10$^{-1}$ |
| 2 | 1.96246 × 10$^{-1}$ |
| 3 | 6.57652 × 10$^{-6}$ |
| 4 | -6.93747 × 10$^{-9}$ |
| 5 | 2.97203 × 10$^{-12}$ |

Enthalpy for water in liquid phase follows

$$H_L = \sum_{n=0}^{6} c_n^{HL} T^n \qquad (4)$$

for 273.15 K $\leq T \leq$ 645 K, while for water in gas phase follows

$$H_G = \sum_{n=0}^{6} c_n^{HG} T^n \qquad (5)$$

for 273.15 K $\leq T \leq$ 640 K. Constants in Equations (4) and (5) are shown in Tables 4 and 5.

Table 4. Constants in Equation (4).

| $n$ | $c_n^{HL}$ |
|---|---|
| 0 | 2.36652 × 10$^4$ |
| 1 | -3.66232 × 10$^2$ |
| 2 | 1.96246 × 10$^{-1}$ |
| 3 | -7.3036 × 10$^{-3}$ |
| 4 | 1.30241 × 10$^{-5}$ |
| 5 | -1.22103 × 10$^{-8}$ |
| 6 | 4.70878 × 10$^{-12}$ |

Table 5. Constants in Equation (5).

| $n$ | $c_n^{HG}$ |
|---|---|
| 0 | -2.20269 × 10$^4$ |
| 1 | 3.65317 × 10$^3$ |
| 2 | -2.25837 × 10$^0$ |
| 3 | 7.37420 × 10$^3$ |
| 4 | -1.33437 × 10$^{-5}$ |
| 5 | 1.26913 × 10$^{-8}$ |
| 6 | -4.9688 × 10$^{-12}$ |

Dynamics viscosity for water in liquid and gas phase can be found through

$$\mu_L = \sum_{n=0}^{6} c_n^{\mu L} T^{-n} \qquad (6)$$

for 273.15 K $\leq T \leq$ 640 K, while for water in gas phase follows

$$\mu_G = \sum_{n=0}^{6} c_n^{\mu G} T^n \qquad (7)$$

for 273.15 K $\leq T \leq$ 645 K. Tables 6 and 7 show constants in Equations (6) and (7).

Table 6. Constants in Equation (6).

| $n$ | $c_n^{\mu L}$ |
|---|---|
| 0 | -1.23274 × 10$^{-2}$ |
| 1 | 2.71038 × 10$^1$ |
| 2 | 2.35275 × 10$^4$ |
| 3 | 1.0425 × 10$^7$ |
| 4 | -2.17342 × 10$^9$ |
| 5 | 1.86935 × 10$^{11}$ |

Table 7. Constants in Equation (7).

| $n$ | $c_n^{\mu L}$ |
|---|---|
| 0 | -5.46807 × 10$^{-4}$ |
| 1 | 6.8949 × 10$^6$ |
| 2 | -3.39999 × 10$^{-8}$ |
| 3 | 8.29842 × 10$^{-11}$ |
| 4 | -9.9706 × 10$^{-14}$ |
| 5 | 4.71914 × 10$^{-17}$ |

Notice that Equations (6) and (7) use power series with different power sign. The former uses negative power sign, while the later uses positive power sign.

*2.2 Mixture of liquid and gas*

Since mixture enthalpy $H_{LG}$ can be measured around the well head, a mixture parameter $x$ can be defined as

$$x = \frac{H_{LG} - H_L}{H_G - H_L}, \qquad (8)$$

where $H_L$ and $H_G$ are obtained from Equations (4) and (5). Mixture mass flow $m$ can also be measured at the same place as $H_{LG}$. Using $x$ and $m$, liquid and gas phase mass flow can be calculated through

$$m_L = m(1 - x) \qquad (9)$$

and

$$m_G = m - m_L = xm. \qquad (10)$$

Using Equations (2) and (3) debit or volumetric flow can be found for liquid and gas phase

$$Q_i = \frac{m_i}{\rho_i} \qquad (11)$$

with $i = L, G$. If pipe diameter is $D$, then cross section area of the pipe will be

$$A = \frac{1}{4}\pi D^2. \qquad (12)$$

Superficial velocity of both phase can be calculated through

$$v_{Si} = \frac{Q_i}{A}, \qquad (13)$$

with $i = L, G$. Mixture density is defined as

$$\rho_n = \rho_L \frac{v_{SL}}{v_m} + \rho_G \frac{v_{SG}}{v_m}. \qquad (14)$$

Substitution of Equations (11) and (13) into Equation (14) will give similar relation to Equation (13), which is

$$v_m = \frac{Q}{A} = \frac{m}{A\rho_n} \qquad (15)$$

mixture velocity.

Surface tension can be predicted using

$$\sigma = 0.2538 \left( \frac{647.15 - T}{647.15} \right)^{1.256 \left[ 1 - \left( \frac{647.15 - T}{647.15} \right) \right]} \qquad (16)$$

for $273.16 \text{ K} \leq T \leq 645.15 \text{ K}$.

There is also another mixture parameter $y$

$$y = \begin{cases} 2.633 \times 10^{-2}, & N_{\text{hold}} < 0.1, \\ \psi \exp \left[ \sum_{n=0}^{4} c_n^y \ln^n N_{\text{hold}} \right], & 0.1 \leq N_{\text{hold}} \leq 4000, \\ \psi, & N_{\text{hold}} > 4000, \end{cases} \qquad (17)$$

which is known as liquid hold up. This parameter is defined as fraction of the pipe element that is occupied by liquid. Constants in Equation (17) are shown in Table 8.

Table 8. Constants in Equation (17).

| $n$ | $c_n^y$ |
|---|---|
| 0 | $-3.6372 \times 10^0$ |
| 1 | $8.813 \times 10^{-1}$ |
| 2 | $-1.335 \times 10^{-1}$ |
| 3 | $1.8534 \times 10^{-2}$ |
| 4 | $-1.066 \times 10^{-3}$ |

Function $N_{\text{hold}}$ in Equation (17) is defined as

$$N_{\text{hold}} = C_N \left( \frac{N_{LV}}{N_{GV}^{0.575}} \right) \left( \frac{p}{1.01325 \times 10^5} \right)^{0.1} \left( \frac{10^6}{N_d} \right), \qquad (18)$$

with liquid velocity number $N_{LV}$, gas velocity number $N_{LG}$, and pipe diameter number $N_D$ are defined as

$$N_{iV} = v_{Si} \left( \frac{\rho_i}{g\sigma} \right)^{\frac{1}{4}}, \qquad (19)$$

with $i = L, G$, and

$$N_D = D \sqrt{\frac{\rho_L g}{\sigma}}. \qquad (20)$$

Function CN in Equation (18) is defined as

$$C_N = \begin{cases} 1.95 \times 10^{-3}, & N_L < 0.002, \\ \exp \left( \sum_{n=0}^{4} c_n^{CN} \ln^n N_L \right), & 0.002 \leq N_L \leq 0.4 . \\ 1.15 \times 10^{-2}, & N_L > 0.4, \end{cases} \qquad (21)$$

where

$$N_L = \mu_L \left( \frac{g}{\rho_L \sigma^3} \right)^{\frac{1}{4}}. \qquad (22)$$

Constants in Equation (21) is given in Table 9.

Table 9. Constants in Equation (22).

| $n$ | $c_n^{CN}$ |
|---|---|
| 0 | $-4.895 \times 10^0$ |
| 1 | $-1.0775 \times 10^0$ |
| 2 | $-8.0822 \times 10^{-1}$ |
| 3 | $1.597 \times 10^{-1}$ |
| 4 | $-1.019 \times 10^{-2}$ |

Function $\psi$ in Equation (17) is defined as

$$\psi = \begin{cases} 1.00, & N_{\text{sec}} > 1, \\ 1 + \exp \left( \sum_{n=0}^{3} c_n^{\psi} \ln^n N_{\text{sec}} \right), & 0.09 \leq N_{\text{sec}} \leq 1, \\ 1.82 & N_{\text{sec}} < 0.09, \end{cases} \qquad (23)$$

with constants is given in Table 10.

Table 10. Constants in Equation (23).

| $n$ | $c_n^{\psi}$ |
|---|---|
| 0 | $6.6598 \times 10^0$ |
| 1 | $8.8173 \times 10^0$ |
| 2 | $3.7693 \times 10^0$ |
| 3 | $5.359 \times 10^{-1}$ |

Function $N_{\text{sec}}$ in Equation (23) is defined as

$$N_{\text{sec}} = \frac{N_{GV} N_L^{0.38}}{N_D^{2.14}} \qquad (24)$$

Then, another mixture density can also be defined

$$\rho_s = y\rho_L + (1 - y)\rho_G, \qquad (25)$$

which is rather different than as in Equation (14). Density in Equation (25) is labeled as mixture density due to liquid hold up impact. Overall mixture density is defined as

$$\rho_f = \frac{\rho_n^2}{\rho_s}. \qquad (26)$$

Using Equation (17) mixture viscosity can be calculated

$$\mu_s = \mu_L^y \mu_G^{(1-y)}, \qquad (27)$$

where both dynamics viscosities, $\mu_L$ and $\mu_G$, are obtained from Equations (6) and (7).

Reynold number in mixture is defined as

$$\text{Re} = \frac{\rho_n v_m D}{\mu_s}, \qquad (28)$$

where laminar flow is for Re < 2000, transition flow for 2000 < Re < 4000, and turbulent flow for Re > 4000. Friction factor $f$ is solution from friction factor equation (Colebrook & White, 1939)

$$\frac{1}{\sqrt{f}} = 1.74 - 2\log\left(\frac{2\varepsilon}{D} + \frac{18.7}{\text{Re}\sqrt{f}}\right), \qquad (29)$$

which holds on the flow through rough pipes that apply to the whole turbulent flow regime, with $\varepsilon$ is absolute roughness.

### 2.3 Pressure drop

In Hagedorn-Brown correlation method three types of pressure drop are considered, i.e. acceleration effect, elevation effect, and friction effect.

Pressure drop due to acceleration effect is defined as

$$\left(\frac{dp}{dz}\right)_a = \frac{1}{2}\rho_s \frac{\Delta v_m^2}{\Delta z}, \qquad (30)$$

with $\Delta z$ is element thickness in $z$ direction.

Pressure drop due to elevation effect is defined as

$$\left(\frac{dp}{dz}\right)_e = g\left[y\rho_L + (1-y)\rho_G\right], \qquad (31)$$

with $g$ is gravitation acceleration.

Pressure drop due to friction is defined as

$$\left(\frac{dp}{dz}\right)_f = \frac{1}{2}\rho_f v_m^2 \frac{f}{D}, \qquad (32)$$

Then, total pressure drop will be

$$\left(\frac{dp}{dz}\right)_t = \left(\frac{dp}{dz}\right)_a + \left(\frac{dp}{dz}\right)_e + \left(\frac{dp}{dz}\right)_f. \qquad (33)$$

Normally, Equation (33) is used to predict pressure-depth profile with mixture information at the well head, e.g. mass flow $m$, velocity $v_m$, and enthalpy $H_{LG}$, In this work it will be used to draw depth-pressure profile below the water level since it also moves with time.

### 2.4 Dynamics of pressure-depth profile

Supposed that in a geothermal well there are only vapor and water with density $\rho_v$ and $\rho_w$, respectively, which is valid that

$$\frac{\rho_w}{\rho_v} \approx 10^2. \qquad (34)$$

Contrast of densities difference will be pronounced in pressure-depth profile ($z$ against $p$) as change in gradient as shown in Figure 1.

Change in gradient indicates position of the volume element (red box), where in the example in Figure 1 position of it is about 1800 m. If vapor above the water level (volume element) is remove, e.g at the well head then the volume element will move with velocity $v_m$ upward. According to pressure drop due to acceleration will increase gradient of vapor part and also of water part as illustrated in Figure 2.
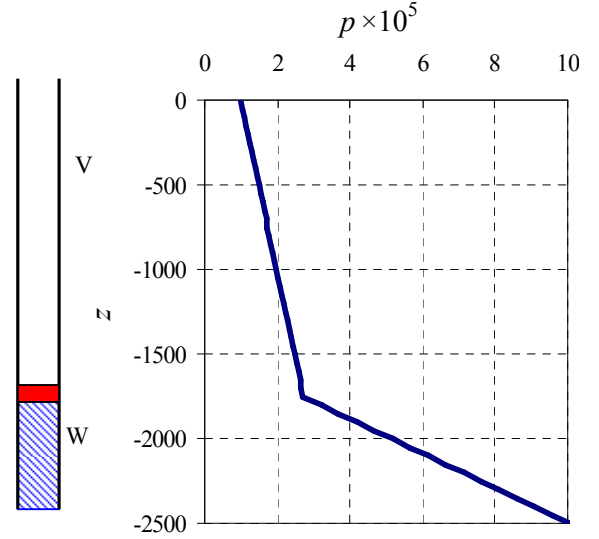


Figure 1. Pressure-depth profile and physical condition of a geothermal well consist of two phases of liquid: vapor (V) and water (W).

Assumed that well head position is at about $z = 0$. As pressure at this point reduced, then vapor will flow upward and then follow by water, which is also moving upward. Figure 2 shows that gradient of the vapor part increase compared to the static condition, and also gradient of the liquid part.
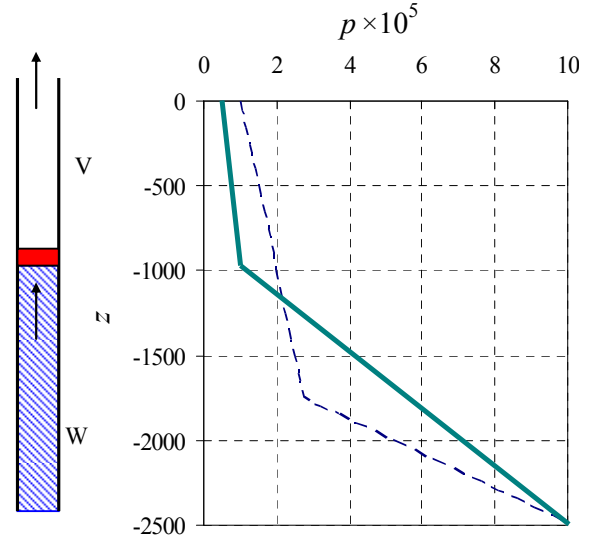


Figure 2. Pressure-depth profile and physical condition of a geothermal well consist of two phases of liquid as vapor (V) and water (W) are moving upward.

Dashed line in Figure 2 indicates static pressure-depth profile previously shown in Figure 1.

For a well that has been successfully discharged, only one gradient of pressure-depth profile will be survived, where mixture information at the well head will be flow mass $m$, mixture parameters $x$ and $y$. Illustration of such flow is given in Figure 3 included by initial static condition and dynamic condition before final steady-state flowing condition has been achieved.

This illustration is not fully right but chosen only for simplicity. It could be that at final steady-state condition not only fluid phase but also small part of vapor can exist.
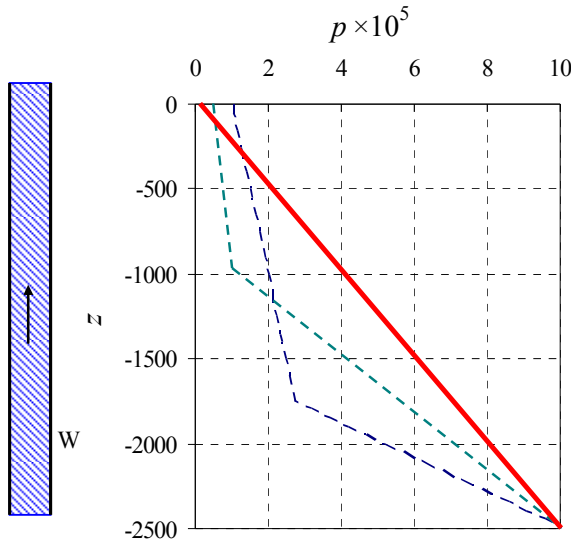
4

Figure 3. Pressure-depth profile at final condition where only fluid phase (W) is flowing.

There is a also assumption that pressure near the feed zone does not change as the well is discharging.

## 2.5 Single fluid volume element (SFVE) method

As previously defined [1] and then implemented in this case [2], SVFE method is based on Newton's second law of motion that uses pressure difference suffered by volume element as driving force. This force at vertical position $z$ can be simply obtained from total pressure difference in Equation (33)

$$\sum F = A\left(\frac{dp}{dz}\right)_{t,z}, \qquad (35)$$

where $A$ is cross section area of the well. Then acceleration of the volume element will be

$$a = \frac{1}{\rho_m A \Delta h}\sum F, \qquad (36)$$

with $\Delta h$ is thickness of fluid volume element in SFVE method. This parameter still can be adjusted to fit observation, when it is necessary. Time integration to obtain velocity and position of fluid volume element is simple Euler method

$$v(t+\Delta t) = v(t) + a\Delta t \qquad (37)$$

and

$$z(t+\Delta t) = z(t) + v(t)\Delta t . \qquad (38)$$

## 3 Results and discussion

Result from implementation only SFVE method and SFVE method accompanied by Hagedorn-Brown method are presented in this part.

## 3.1 Unrealistic results from previous work (SFVE only)

Simulation parameters are $\Delta h = 10$ m and $\Delta t = 10^{-4}$ s, with range of $\rho_0$ (1 - 40 kg/m$^3$) in order to match observation data for flow occurrence at the two wells [3], where the results are given in Figure 4.

It is found that the cross over line between the flow and no flow states is located between values $\rho_0 = 28$ kg/m$^3$ and $\rho_0 = 28.5$ kg/m$^3$ for the well PAL-9D, while for the

well PAL-1RD all variations of $\rho_0$ give no flow. Observation results give flow occurrence for PAL-9D and no flow for PAL-1RD. This means that this method produces results that match observation only for values 1 kg/m$^3$ < $\rho_0$ < 28 kg/m$^3$, which is the density rather for vapor (0.8 kg/m$^3$) than water (1000 kg/m$^3$). Single-phase fluid is determined using following relation

$$\rho(T,p) = \frac{\rho_0}{\left[1+\beta(T-T_0)\right]\left[1-(p-p_0)/E\right]}. \qquad (35)$$

as used in [2].

If single-phase density can be defined simply through

$$\rho_o = \alpha\rho_{\text{water}} + (1-\alpha)\rho_{\text{vapor}} \qquad (36)$$

or

$$\alpha = \frac{\rho_o - \rho_{\text{vapor}}}{\rho_{\text{water}} - \rho_{\text{vapor}}}, \qquad (37)$$

then value of $\alpha$ is between $2\times10^{-4}$ and $2.72\times10^{-2}$ for the previous range of $\rho_0$. It is a very vapor-rich mixture of water-vapor. In this work Equation (37) is labeled as density fraction for water.

Time required for flow to occur as observed in well head is about 80 s simulation time, which is too short comparing to real required time about a couple of hours.
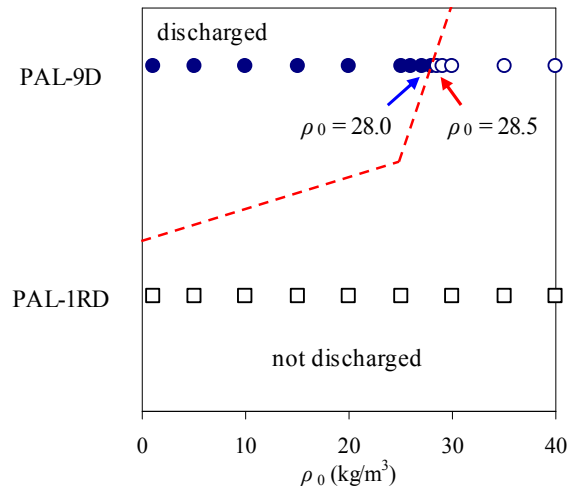


Figure 4. Flow occurrence as function of $\rho_0$ for the two wells in [3] using only SFVE method.

This unrealistic result that density of the discharged fluid is too light and discharge time is too short shows that implementation of SFVE only, which is considering single-phase fluid, does not work well. Advancement of this method is by considering two-phase flow through Hagedorn-Brown method. The unrealistic result can also be addressed to static pressure-depth profile, which should be changed during performing the SFVE.

## 3.2 SVFE-HB method

Implementation of single fluid volume element - Hagedorn-Brown (SFVE-HB) method is performed in two ways. The first is conducting only HB correlation method in predicting pressure-depth profile in flowing condition with requirement that recharge mass flow should be equal or less than feed zone mass flow. The second is implementing HB method in SVFE and

obtaining dynamics of pressure-depth profile. When the well discharges then its final pressure-depth profile should match the depth-profile obtained from HB correlation method. If the well does not discharge the profiles can not be compared to each other.

## 4 Conclusion

Implementation of SFVE method only in two geothermal wells gives range of single-phase fluid between 1 - 28 $kg/m^3$, which could be too light for water-vapor mixture, where the density fraction is between $2\times10^{-4}$ and $2.72\times10^{-2}$ for water. Recharge time is about 80 s or less, which is too short compared to a couple hours as observed. SFVE-HB method can produce the dynamics of pressure-depth profile that matches the profile obtained using HB correlation method if the well discharges.

## Acknowledgement

## References

[1]  S. Viridi, Novitrian, Nuhayati, W. Hidayat, F. D. E. Latief, and F. P. Zen, "Development of Single Fluid Volume Element Method for Simulation of Transient Fluid Flow in Self-Siphons", AIP Conference Proceedings 1615, 199-207 (2014).

[2]  S. Viridi and Y. Windra, "Implementation of Single Fluid Volume Element Method in Predicting Flow Occurrence of One-Dimensional Geothermal Well", viXra:1504.0201, 2015-04-26.

[3]  F. X. M. Sta. Ana, "A Study on Simulation by Air Compression on Some of the Philippine Geothermal Wells", Geothermal Institute, University of Auckland, Australia, October 1985.